ELSEVIER

Journal of Nuclear Materials 294 (2001) 88–93

journal of nuclear materials

www.elsevier.nl/locate/jnucmat

Selected thermal properties of beryllium and phase equilibria in beryllium systems relevant for nuclear fusion reactor blankets

Heiko Kleykamp *

Forschungszentrum Karlsruhe, Institut für Materialforschung I, Postfach 3640, 76021 Karlsruhe, Germany

Abstract

Enthalpies of the hcp–bcc transformation $\Delta_{tr}H$ and melting $\Delta_{m}H$ of Be were measured by anisothermal calorimetry which gave $\Delta_{tr}H = 6100$ J/mol and $\Delta_{m}H = 7200$ J/mol. The high value of $\Delta_{tr}H$ is explained by the strongly reduced c/a-axis ratio of the hcp modification. Maximum solubilities of the metallic impurities Al, Cr, Fe, Mg and Si in different Be qualities which annealed at about 800°C are 0.01 mol% or less in each case. In the Al–Be–Fe system, Be(Al, Fe) is in equilibrium with Al_5Fe_2 at 870°C. The phases $AlFeBe_4$ and $Al_2FeBe_{2.3}$ were not observed. The Be–C–Si system is marked by two two-phase equilibria Be_2C–Si and Be_2C–SiC at 900°C. The phase diagram of the pseudo-ternary BeO–Li_2O–SiO_2 system was established on the basis of in-pile Be–BeO–Li_4SiO_4–Li_2SiO_3 compatibility studies at about 450°C. The system is characterised by Li_2BeSiO_4 which is in equilibrium with BeO, Be_2SiO_4, SiO_2, $Li_2Si_2O_5$, Li_2SiO_3 and Li_4SiO_4. The latter phase is also in equilibrium with $Li_2Be_2O_3$.

1. Introduction

Beryllium is a main group metal of high affinity to oxygen, is very brittle and possesses high hardness. A structural hcp–bcc transformation occurs 15 degrees below melting. Beryllium is used for X-ray windows, for electrical contacts and electrodes and for neutron generation sources. Be oxide refractories are recommended at high temperatures. Alloys with Al, Cu, Ni, etc. are utilised, e.g., for watch springs, surgical instruments and brakes in astronautics. Beryllium is further designated in nuclear fusion technology for protective coatings and evaporators in the plasma torus and as neutron multiplier in the breeding blanket of future reactors. For the latter application, the neutron flux is increased by the prominent inelastic nuclear reaction

$$^{9}\mathrm{Be} + n = 2n + {}^{8}\mathrm{Be}. \quad (1)$$

above the threshold energy of 2.7 MeV with the subsequent decay of ^{8}Be into two α-particles. The increased neutron flux enhances tritium breeding in the lithium-containing blanket according to the (n, α)-reaction

$$^{6}\mathrm{Li} + n = \alpha + {}^{3}\mathrm{H}. \quad (2)$$

Due to these high-temperature uses of beryllium the revision of some thermal properties and phase equilibria with other materials of technological interest is indicated.

2. Experimental

2.1. Equipment

Measurements of transformation and melting enthalpy of beryllium were carried out by a high-temperature calorimeter (HTC 1800, Setaram S.A., Lyon, France) which was used anisothermally in the heating mode according to the heat flux principle. As the time constant of the signals is high ($\tau_1 = 5$ min), special care was taken to separate adjacent peaks. The temperatures of transformation and melting of beryllium were determined more reliably by differential thermal analysis (DTA) with a short time constant $\tau_1 < 0.5$ min. Details of the calibration are given in [1,2].

* Tel.: +49-7247 82 2888; fax: +49-7247 82 4567.

E-mail address: heiko.kleykamp@imf.fzk.de (H. Kleykamp).

0022-3115/01/$ - see front matter
PII: S0022-3115(01)00442-1

Annealings of beryllium-containing samples encapsulated in molybdenum for phase equilibria and compatibility studies were made in a standard furnace under purified argon. Metallographic and ceramographic preparations, however, were performed in glove boxes. The irradiated material was handled in lead-shielded 'hot cells' and analysed in shielded instruments.

The wavelength dispersive X-ray microanalysis was used to characterise beryllium in micrometer scales in order to support the quality control of commercially available beryllium, the investigation of phase equilibria studies in multi-component beryllium systems and the compatibility of beryllium with other materials. A commercial synthetic Mo–B_4C multilayer X-ray diffracting device with $2d = 22.2$ nm periodicity was used to extend the X-ray microanalysis to the ultra-light element beryllium in an existing shielded instrument. The modified spectrometer covered a wavelength range between 5.2 and 13 nm. The wavelength of the Be Kα emission line from elemental Be was measured to be $\lambda = 11.35$ nm (=109.2 eV) and the full width at half-maximum was 7.2 eV which is sufficient for the separation of the Be Kα line from higher-order emission lines of heavy elements [3]. Since the mass absorption coefficients of the Kα lines of the elements of interest, Mg to Ni, in Be are low (about 100 cm^2/g) compared to those of the Be Kα line in the said elements (up to the order of 100000 cm^2/g) [4], very low concentrations of impurities can be detected in Be, down to 0.01 mass% or even lower.

2.2. Materials

The transformation and melting enthalpy measurements were made by the use of thin beryllium discs (mass about 50 mg) with 8 mm diameter which covered the flat bottom of the Al_2O_3 crucibles of the calorimeter. The material (Heraeus, Hanau, Germany) had been extracted and hot-rolled from vacuum-melted and electrolytically refined beryllium, see Table 1.

The isothermal section of the ternary Be–C–Si system was investigated in the course of Be–SiC compatibility studies with SiC–Be–SiC pellet stacks. Beryllium discs (Heraeus) and β-SiC pellets (Elektroschmelzwerk Kempten, Kempten, Germany) were used. The reaction products were analysed by ceramography, microhardness measurements, X-ray microanalysis and X-ray diffraction [5].

Beryllium pebbles (Brush Wellman, Cleveland, USA; NGK Insulators, Handa City, Japan) had been fabricated by the magnesium reduction process without further refinement or by successive vacuum melting to remove magnesium impurity phases [3]. The chemical analysis of the suppliers is given in Table 1. As-fabricated, annealed and irradiated pebbles were examined by X-ray microanalysis to determine the number density and composition of precipitates which might influence the integrity of the pebbles during irradiation.

Lithium orthosilicate pebbles (Schott, Mainz, Germany) were manufactured under an argon atmosphere by spraying a melt jet which had passed a narrow nozzle [6]. A mixture of Li_4SiO_4 and beryllium pebbles was irradiated in one capsule of the EXOTIC-7 experiment in the high-flux reactor Petten up to 18% lithium burnup [7]. The reaction products between Li_4SiO_4 and Be initially present were Li_2SiO_3, BeO, Li_2BeSiO_4 and $Li_2Be_2O_3$ which were used to establish a phase diagram of the pseudo-ternary BeO–Li_2O–SiO_2 system.

Table 1
Typical concentrations of impurities in beryllium fabricated by different methods and used in this study, in mass%

Supplier:	Heraeus	NGK	Brush Wellman	Brush Wellman
Fabrication method:	Vacuum melting, electrolytic refinement	Vacuum melting, rot. electr. proc.	Vacuum melting, melt atomising	Mg reduction of BeF_2, intermediate product
Al	0.01	0.038	0.04	0.025–0.035
C	0.03	–	0.07	0.045
Cl	–	–	$\leqslant 0.01$	–
Cr	0.003	–	–	0.011–0.015
F	–	–	$\leqslant 0.008$	0.06–0.18
Fe	0.03	0.066	0.09	0.05–0.07
Mg	0.006	0.024	$\leqslant 0.01$	0.12–0.16
Mn	0.003	0.010	–	0.01
O	0.02	0.16	0.22	0.05–0.20
N	–	–	–	0.021
Ni	0.02	–	–	0.01
Si	0.01	0.023	0.03	0.02–0.03
U	–	<0.01	0.0023	0.013–0.015
Zr	–	–	–	0.013–0.021
Others	<0.04	–	–	–
Be	>99.83	99.67	$\simeq 99.5$	$\simeq 99.3$

Table 2
Enthalpies of transformation $\Delta_{tr}H$ and melting $\Delta_{m}H$ of beryllium

$\Delta_{tr}H$ in J/mol	$\Delta_{m}H$ in J/mol	$\Delta_{tr}H + \Delta_{m}H$	Method	Year	Reference
–	–	14 800	drop calorimetry	1960	[8]
7500	14600	(22 100)	Clausius–Clapeyron $(T_{tr}, T_{m}) = f(p)$	1965	[9]
–	−9050[a]	–	anisothermal calorimetry	1972	[10]
2100	2400	(4500)	DTA (peak area integration)	1977	[11]
7950	9200	(17 150)	DTA (peak area weighing)	1984	[12]
6100 ± 500	7200 ± 500	(13 300)	anisothermal calorimetry	2000	[1,2]

[a] Enthalpy of solidification.

3. Results and discussion

3.1. Thermal properties of beryllium

The DTA results of beryllium revealed two peaks which were completely separated from each other by 15 degrees and could be related to the hcp–bcc transformation and to the melting process of this metal. The first peak started at (1268 ± 1)°C by a sharp increase from the base line and is attributed to the transformation temperature. The second peak left the base line by a bent curve and passed over to a linear curve. The transition in this curve was characterised by a distinct bend at (1283 ± 2)°C which is the melting temperature [1,2].

The enthalpy of transition of beryllium (the sum of the enthalpies of transformation $\Delta_{tr}H$ and melting $\Delta_{m}H$) was determined by drop calorimetry [8]; $\Delta_{tr}H$ and $\Delta_{m}H$ were calculated from the pressure dependence of the transformation and melting temperatures [9]; $\Delta_{m}H$ was evaluated further from anisothermal calorimetry in the cooling mode [10]; and $\Delta_{tr}H$ and $\Delta_{m}H$ were determined by peak quantification of differential thermal analysis [11,12]. The results are compiled in Table 2.

Enthalpies of transformation and melting of beryllium were measured in this work by the heats Q (given in μV s) consumed or released by the transition process according to $Q = S\Delta H\, m/M$, where S (given in μV/mW) is the sensitivity factor, ΔH is the molar enthalpy of transition, M is the molar mass and m is the mass of the sample. The double-peak area Q in Fig. 1 was divided into two single-peak areas $Q_{tr} + Q_{m} = Q$ by a programmed vertical line at the position of the local maximum of the curve. As a result of five measurements the ratio of the peak areas of the enthalpy of melting and the enthalpy of transformation is $Q_{m}/Q_{tr} = 1.17 \pm 0.01$. The calorimeter was calibrated at a heating rate of 2 K/min with the enthalpies of melting of gold and nickel [13] using three specimens of each metal and different masses for each specimen. The temperature-dependent sensitivity factor revealed $S = (0.535 \pm 0.016)$ μV/mW at 1064.4°C (gold) and $S = (0.328 \pm 0.014)$ μV/mW at 1455.2°C (nickel). The factor interpolated at 1276°C, the average temperature between transformation and melting of beryllium, is $S_{Be} = (0.423 \pm 0.021)$ μV/mW. The heat flow on the right ordinate of Fig. 1 divided by S gives directly the power in mW. The enthalpies of transformation and melting of beryllium, including the statistical errors, yield $\Delta_{tr}H = (6149 \pm 437)$ J/mol and $\Delta_{m}H = (7194 \pm 512)$ J/mol, respectively.

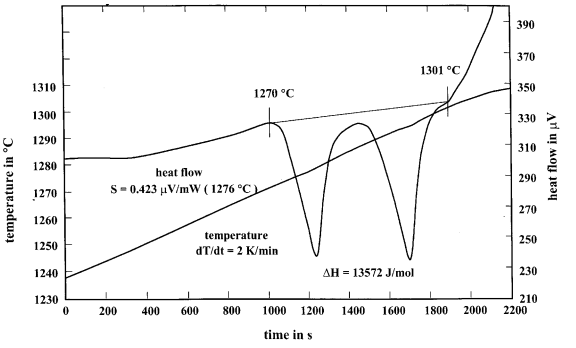

Fig. 1. Enthalpies of transformation $\Delta_{tr}H$ and melting $\Delta_{m}H$ of beryllium measured by anisothermal calorimetry. The peak-area ratio is $\Delta_{m}H : \Delta_{tr}H = 1.17$ [1,2].

The enthalpy of transformation of beryllium is extremely high compared to the enthalpy of melting and is higher than the known enthalpies of transformation of other elements transforming from the hcp to the bcc crystal structure with increasing temperature [13]. A reason might be the very compressed c/a-axis ratio of beryllium with $c/a = 1.567$ compared to the ideal ratio $c/a = 1.633$. The enthalpy of transformation of elements is plotted as a function of the c/a-axis ratio in Fig. 2. The stronger the deviation of this ratio from the ideal ratio, the higher the enthalpy of transformation which can be split into two terms: (1) energy of stretching of the c-axis to the ideal c/a-ratio which is the major part of the enthalpy of transformation, (2) energy of transforming the ideal hcp lattice in first co-ordination by destroying the arrangement of the nearest neighbours and rearrangement of the new bcc lattice with a different co-ordination number.

The technical implication of the bcc–hcp re-transformation of beryllium during the processing is the very

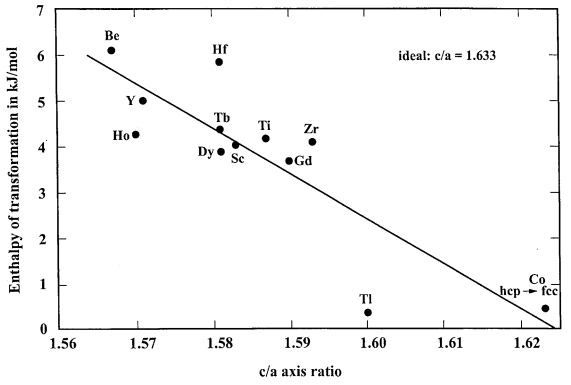

Fig. 2. Enthalpy of the hcp–bcc transformation as a function of the c/a-axis ratio of the hexagonal modification of the elements.

high heat release yielding a specific value of −677 J/g at 1268°C. This value is by more than one order of magnitude higher than the specific enthalpy of the bcc–hcp re-transformation of zirconium yielding −45 J/g [13]. The manufacture of the elements is a typical example of the Kroll process which is characterised by the reduction of their fluorides and chlorides with magnesium.

3.2. Solubility of metallic elements in beryllium

The maximum solubilities of metallic elements in beryllium are very low and are in most cases under the detection limit of conventional methods. Higher solubilities in the 1 at.% range were reported for the elements Co, Ni, Cu, Pd and Pt [14]. Concentrations of the impurities listed in Table 1 are mostly above their solubility limits. Selected metallic elements dissolved in the beryllium matrix were investigated by X-ray microanalysis under optimised conditions, e.g., at higher working voltage, which improves the detection limits. The elements Al, Cr, Fe, Mg and Si were found in measurable concentrations in the Be matrix, which are the maximum solubilities in the multi-component system, annealed at 870°C and subsequently down to 690°C, see Table 3. The maximum solubilities are expected to be slightly different in the respective binary beryllium systems.

Numerous precipitates were observed and quantitatively analysed in beryllium that had been prepared by the magnesium reduction process. Pebbles annealed from 790°C down to 690°C and beryllium neutron-irradiated in the HFR (Be/Pe experiment) up to 2×10^{25} n/m^2 ($E > 0.1$ MeV) and thereupon annealed at 650°C show the following precipitates: $MgBe_{13}$, $(Mg, Zr, U)Be_{13}$, Mg_2Si, Al_3Mg_2 and Be_2C as well as Fe–Cr and Al–Cr–Mg phases. X-ray diffraction of the most frequently observed phase $MgBe_{13}$ yielded the cubic $NaZn_{13}$-type structure with the measured lattice parameter $a = (1016 \pm 1)$ pm. Vacuum melting of beryllium evaporated magnesium. This effect resulted in a lower amount of precipitates which are free of magnesium. Beryllium prepared by this method contained the following precipitates: Al_5Fe_2, graphite, SiC and Fe–Cr alloys. Annealings at 870°C and thereupon at lower temperatures down to 690°C resulted in the equilibrium phases Al_5Fe_2, Be_2C and Fe–Cr silicides. SiC has a relatively low thermodynamic stability and reacts with the Be matrix to Be_2C (see Section 3.4), Si forms silicides with the Fe–Cr impurities. The formation of low-melting Al–Mg alloys can be avoided by the presence of silicon that is not dissolved in Be and not bonded to transition metal silicides. The Si/Mg atomic ratio of these components beyond their solubility limits in Be should be higher than 0.5. Thus, the formation of high-melting Mg_2Si is warranted in equilibrium with Si or other silicides.

Table 3
Maximum solubility of metallic impurities in beryllium after annealing under helium at 870°C and subsequently down to 690°C, measured in mass%

Element	Max. solubility	
	mass%	at.%
Al	0.029	0.010
Cr	0.01	0.002
Fe	0.06	0.010
Mg	<0.01	<0.004
Si	0.019	0.006

3.3. The Al–Be–Fe system

Aluminium and iron are the main metallic impurity elements in beryllium purified by vacuum melting. Therefore, reconsiderations on the ternary Al–Be–Fe system are indicated. The Be apex of the isothermal section of the system based on annealings between 800 and 850°C was reported in [15], see Fig. 3. At 800°C the maximum solubility of Al in Be is 0.007 at.%, of Fe in Be is 0.11 at.%. In the ternary, Be(Al, Fe) with 0.02 at.% Al and varying Fe concentrations between 0.01 and 0.08 at.% Fe is in equilibrium with $AlFeBe_4$ [15]. This phase decomposes at 850°C or slightly above this temperature [16]. A second ternary phase $Al_2FeBe_{2.3}$ was reported in [17].

The ternary phases in beryllium purified by vacuum melting and annealed at 870°C and subsequently down to 690°C could not be observed in this study. Be(Al, Fe) with 0.01 at.% Al and 0.01 at.% Fe in the Be matrix was observed to be in equilibrium with Al_5Fe_2. To avoid the formation of liquid Al(Be) in Be(Al, Fe) above the eutectic temperature 644°C in the Al–Be system, an atomic ratio Fe/Al > 1 (mass ratio Fe/Al > 2) is recommended as the Al and Fe impurity concentration ratio in beryllium for neutron multiplier applications.

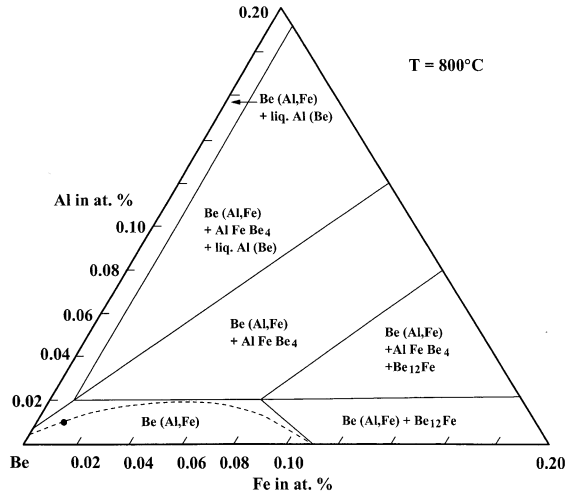

Fig. 3. Isothermal section of the Be apex of the Al–Be–Fe system at 800°C [15]. The experimental point is from this study.

3.4. The Be–C–Si system

The reaction kinetics between Be and SiC has been investigated by diffusion couple experiments in order to study the compatibility between the neutron multiplier beryllium and SiC fibre-reinforced SiC foreseen as a structural material for the fusion reactor. The system is incompatible above 700°C, a Be_2C–Si layer is formed between SiC and Be. The increase of the layer thickness obeys a parabolic time law [5]. An isothermal section of the phase diagram of the ternary Be–C–Si system at 900°C could be established from these observations. Phase equilibria exist between Be_2C and Si and between Be_2C and SiC [5]. The maximum solubility of Be in Si at 900°C is below the detection limit of 0.6 at.% Be, that of Si in Be is about 0.006 at.% Si measured by X-ray microanalysis, see Table 3. An equivalent isothermal section of the Be–C–Si system at 1000°C was published earlier [18].

3.5. The BeO–Li_2O–SiO_2 system

The knowledge of the reaction behaviour between Be, Li_4SiO_4, Li_2SiO_3 and BeO is the basis for the selection of a thermodynamically stable neutron multiplier – tritium breeding material system. Out-of-pile compatibility studies between beryllium and Li_4SiO_4 under argon have shown a reaction layer of about 10 μm thickness and unknown composition at 650°C after 1000 h reaction time [19]. According to the calculated phase diagram of the quaternary Be–Li–O–Si system the formed reaction products between Be and Li_4SiO_4 should be BeO, $Li_2Be_2O_3$ and Li_2Si [20].

The situation is different under neutron irradiation. The compatibility of Be with Li_4SiO_4 was studied in an early irradiation experiment. A mixture of Be and Li_4SiO_4 (+2 mass% SiO_2) pebbles in ferritic steel capsules was irradiated under a He – 0.1 vol.% H_2 atmosphere up to 18% Li burnup for one year in the quoted temperature interval 410–480°C [21]. Detailed post-irradiation studies of this EXOTIC-7 experiment by X-ray microanalysis gained insight into the phase equilibria of the Be–Li–O–Si system [7]. Part of Li_4SiO_4 reacted to Li_2SiO_3 due to the Li transmutation according to Eq. (2), and the released oxygen oxidised Be to BeO. This reaction behaviour can be formulated after 18% Li burnup by

$$100Li_4SiO_4 + 36Be = 64Li_4SiO_4 + 36Li_2SiO_3 + 72He + 36T_2 + 36BeO. \quad (3)$$

BeO on the surface of the Be pebbles reacted with the Li_4SiO_4–Li_2SiO_3 pebbles in direct contact by a secondary reaction according to

$$BeO + Li_2SiO_3 = Li_2BeSiO_4. \quad (4)$$

In parallel, the formation of $Li_2Be_2O_3$ was observed between Be and Li_4SiO_4 by the reaction

$$3Be + Li_4SiO_4 = BeO + Li_2Be_2O_3 + Li_2Si. \quad (5)$$

The reaction products BeO and $Li_2Be_2O_3$ could be detected by X-ray microanalysis. Unfortunately, the composition Li_2Si could not be proven. The phase equilibria according to Eq. (5) are in accordance with the calculated quaternary system [20]. The reaction behaviour of the Be–BeO–Li_4SiO_4–Li_2SiO_3 system under irradiation and the quantitative analysis of the formed phases result in an isothermal section of the pseudo-ternary BeO–Li_2O–SiO_2 system at about 450°C which is illustrated in Fig. 4. The system is characterised by the quaternary oxide Li_2BeSiO_4 which is in equilibrium with Be_2SiO_4, BeO, Li_4SiO_4, Li_2SiO_3 and probably with

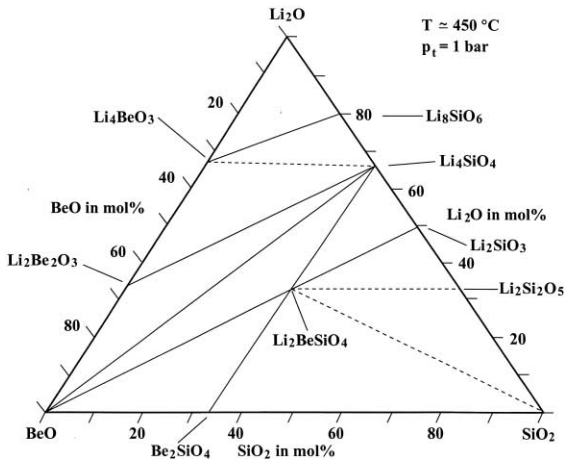

Fig. 4. Isothermal section of the phase diagram of the BeO–Li_2O–SiO_2 system at about 450°C. Experimental data from [7].

$Li_2Si_2O_5$ and SiO_2. Further, Li_4SiO_4 is in equilibrium with BeO, $Li_2Be_2O_3$ and probably with Li_4BeO_3.

4. Conclusions

Beryllium has an hcp–bcc transformation 15 degrees below its melting point at 1283°C. The enthalpy of transformation is uncommonly high which might influence the Be process metallurgy, and is explained by the compressed c/a-axis ratio of the hcp cell. The main metallic impurities in vacuum-melted beryllium are Al, Fe, Mg and Si. The Fe/Al mole ratio should be higher than one in order to avoid liquid Al precipitates in the Be matrix above the eutectic temperature at 644°C. The Mg/Si mole ratio should be optimised in order to avoid liquid Al–Mg phases above 400°C which might influence the mechanical behaviour of beryllium. Be and SiC are incompatible above about 700°C by formation of stable Be_2C and Si. The use of Be and Li_4SiO_4 in one common container of fusion blanket material irradiations is not advisable as a result of chemical interactions in the BeO–Li_2O–SiO_2 system.

References

[1] H. Kleykamp, Thermochim. Acta 345 (2000) 179.
[2] H. Kleykamp, Netsu Sokutei 27 (2000) 100.
[3] H. Kleykamp, J. Anal. At. Spectrom. 14 (1999) 377.
[4] B.L. Henke, E.S. Ebisu, At. Data Nucl. Data Tables 27 (1982) 1.
[5] H. Kleykamp, J. Nucl. Mater. 283–287 (2000) 1385.
[6] H. Kleykamp, Thermochim. Acta 287 (1996) 191.
[7] H. Kleykamp, J. Nucl. Mater. 273 (1999) 171.
[8] P.B. Kantor, R.M. Krasovitskaya, A.N. Kisel, Phys. Met. Metallogr. 10 (6) (1960) 835.
[9] M. Francois, M. Contre, in: Proceedings of International Conference on Beryllium, Grenoble, Presses Univ. de France, Paris, 1965, p. 201.
[10] A. Radenac, C. Berthaut, High Temp. High Press. 4 (1972) 485.
[11] R.G. Loasby, D. Dearden, J. Less-Common Met. 52 (1977) 137.
[12] A. Abey, Report UCLR-53567, 1984.
[13] A.T. Dinsdale, NPL report DMA (A) 195, 1989.
[14] T.B. Massalski, Binary Alloy Phase Diagrams, 2nd Ed., ASM, Metals Park, OH, 1990.
[15] S.M. Myers, J.E. Smugeresky, Metall. Trans. A 9 (1978) 1789.
[16] H.P. Rooksby, J. Nucl. Mater. 7 (1962) 205.
[17] P.J. Black, Acta Crystallogr. 8 (1955) 39.
[18] N.N. Matyushenko, A.A. Rozen, N.S. Pugachev, Sov. Powder Metall. Met. Ceram. 5 (1966) 310.
[19] P. Hofmann, W. Dienst, J. Nucl. Mater. 171 (1990) 203.
[20] H. Migge, in: Proceedings of 14th Symposium on Fusion Technology, Avignon, 1986, p. 1209.
[21] J.G. von der Laan, H. Kwast, M. Stijkel, R. Conrad, R. May, S. Casadio, N. Roux, H. Werle, R.A. Verrall, J. Nucl. Mater. 233 (1996) 1446.